LITERATURE CITED

1. Tables of Standard Handbook Data: Dynamic Viscosity and Thermal Conductivity of Helium, Neon, Argon, Krypton, and Xenon at Atmospheric Pressure at Temperatures from Normal Boiling Points to 2500°K [in Russian], Moscow (1982).
2. Tables of Standard Handbook Data: Nitrogen, Second Virial Coefficient, Coefficients of Dynamic Viscosity, Thermal Conductivity, and Self-Diffusion of a Rarefied Gas in the Temperature Range 65-2500°K [in Russian], Moscow (1984).
3. E. Vogel, Phys. Chemie, 88, No. 10, 997-999 (1984).
4. J. H. Dymond and E. B. Smith, The Virial Coefficients of Pure Gases and Mixtures. A Critical Compilation, Oxford (1980).
5. R. M. Sevast'yanov and N. A. Zykov, Inzh.-Fiz. Zh., 38, No. 4, 639-643 (1980).
6. N. A. Zykov, R. M. Sevast'yanov, and R. A. Chernyavskaya, Inzh.-Fiz. Zh., 44, No. 3, 447-451 (1983).
7. A. Michels, T. Wassenaar, and G. Wolkers, Physica, 31, 237-250 (1965).
8. A. Michels, Hub Wijker,and Hk. Wijker, Physica, 15, 627-649 (1949).
9. N. Trappeniers, T. Wassenaar, and G. Wolkers, Physica, 32, 1503-1520 (1966).
10. V. A. Rabinovich, A. A. Vasserman, V. I. Nedostup, and L. S. Veksler, Thermophysical Properties of Neon, Argon, Krypton, and Xenon [in Russian], Moscow (1976).
11. N. A. Zykov, R. M. Sevast'yanov, and R. A. Chernyavskaya, Inzh.-Fiz. Zh., 47, No. 1, 108-111 (1984).

EFFECT OF THE CHARACTERISTIC MAGNETIC FIELD OF A HIGH-CURRENT ELECTRON BEAM ON ENERGY RELEASE IN TARGETS

G. E. Gorelik, S. I. Legovich, and S. G. Rozin

UDC 537.533.7

The character of the energy released by a high-current electron beam in metal targets is studied taking into account the self-action of the beam.

When an electron beam interacts with a metal barrier, matter is heated, melted, evaporated, and dispersed. The flow of the indicated processes is largely determined by the character of the energy release by fast electrons, i.e., the heat source, forming in the material. The distribution of energy losses by weak-current electron beams is usually calculated using the linear single-electron approximation [1, 2], when only the interaction of fast electrons in the beam with atoms and electrons in the material is taken into account. As experiments have demonstrated [3, 4], for high-current electron beams (HCEB, $I \geqslant 10$ kA), compared with weak-current beams, it is observed that the penetration depth of the electrons in the target decreases, energy release in thin targets increases, and the heating is more intense. To explain these facts the high-current electron beam must be regarded as a flux of charged particles, whose evolution is determined by the characteristic electromagnetic fields [5], i.e., it is necessary to take into account in addition (compared with the weak-current beam) the interaction of fast electrons in the beam with one another via the characteristic fields.

This paper is devoted to the study of the effect of the characteristic magnetic field of HCEB on the energy released in Al, Cu, and Au targets. The basic assumptions made in formulating the problem and the methodology are analogous to those presented in [6]:

1) since the relaxation time of a fast electron is much shorter than the characteristic time over which the parameters of the beam change, the kinetic equation is solved in the quasistationary approximation;

2) because of the high conductivity of the plasma formed the electric field of the thermalized electrons is neglected; and,

---

A. V. Lykov Institute of Heat and Mass Transfer, Academy of Sciences of the Belorussian SSR. Institute of Nuclear Power, Academy of Sciences of the Belorussian SSR, Minsk.

Translated from Inzhenerno-Fizicheskii Zhurnal, Vol. 52, No. 6, pp. 977-980, June, 1987. Original article submitted April 1, 1986.

0022-0841/87/5206-0705 $12.50

3) assuming that there are no eddy currents (the target is represented by a collection of thin foils, oriented perpendicular to the beam) the magnetic field rapidly penetrates into the absorber, so that it has a maximum effect, as compared with a continuous absorber, and the nonstationary terms in the corresponding Maxwell's equation can be neglected.

Thus, under the assumptions made the self-consistent problem of absorption of HCEB in targets reduces to the simultaneous solution of the kinetic equation for transport of relativistic electrons in the beam and Maxwell's equations for the characteristic magnetic field of the beam.

The problem was solved by the method of iterations in two stages: the trajectories were calculated in a fixed field and the fields were calculated based on the computed trajectories. The iteration process terminated when the difference between the values of the density of energy losses in subsequent iterations becomes less than a fixed value.

The trajectories of the electrons in the beam were calculated by the Monte Carlo method using the scheme of continuous energy losses and scattering on a segment based on the Goudsmith–Saunderson formulas [2]. The minimum tracking energy was chosen so that the electron range $r_0(E_{min})$ would be less than one-half the grid step h (cell size). The effect of the magnetic field was taken into account by additionally varying the momentum of the particle at the end of the segment in accordance with the solution of the relativistic equation of motion of an electron:

$$m\frac{d}{dt}(\gamma\boldsymbol{\beta}) = -e\,[\boldsymbol{\beta}\mathbf{B}], \tag{1}$$

which under the assumption that the velocity is constant on the segment gives relations between the direction of the particle at the beginning (index 0) and end (index 1) of the step:

$$\begin{aligned} (\gamma\beta_r)_1 &= (\gamma\beta_r)_0\cos b - (\gamma\beta_z)\sin b, \\ (\gamma\beta_\varphi)_1 &= (\gamma\beta_\varphi)_0, \\ (\gamma\beta_z)_1 &= (\gamma\beta_z)_0\cos b + (\gamma\beta_r)\sin b, \end{aligned} \tag{2}$$

where $\beta(\beta_r, \beta_\varphi, \beta_z) = v/c$ is the relative velocity of an electron in a cylindrical coordinate system; $\gamma = (1 = v^2/c^2)^{1/2}$; B is the magnetic induction vector; $b = (eBs/mc\gamma\beta)$ is the effective angle of deflection in the magnetic field for a step of size s. The value of s was chosen from the condition that the energy losses be small ($\Delta E = 0.01E$) and the angle of deflection of the electron is a step be limited ($b < 1$ rad). It was assumed that the electrons emerging from the target are returned by the diode field.

It should be noted that for the axisymmetric case only the azimuthal component of the magnetic field B_φ, determined by the longitudinal component of the current density vector J_z, need be taken into account. For the calculations the grid was divided into cells bounded by the surfaces of a cylindrical coordinate system $r = r_j = jh$, $z = z_i = ih$, $h = r_0/15$. The mean azimuthal field in a cell (ij) was determined from the total current law [7]:

$$B_{\varphi ij} = \frac{\mu\mu_0 h}{2j+1}\sum_{j=1}^{j}(2j+1)\,J_{zij}, \tag{3}$$

where μ_0 is the magnetic permeability of the vacuum; μ is the relative magnetic permeability of the medium; J_{zij} is the projection of the mean current density of the beam in the ij cell, which is determined by the method of current tubes [6]:

$$J_{zij} = \frac{I}{\pi N h^3(2j+1)}\sum_{k=1}^{N} l_{ij}^{(k)}\cos\theta_{ij}^{(k)}, \tag{4}$$

on the z axis. Here $l_{ij}^{(k)}$ is the length of the trajectory of the k-th particle in the ij cell; I is the beam current; N is the number of large particles in the beam; and $\theta_{ij}^{(k)}$ is the angle formed with the velocity vector of the k-th particle in the cell (ij).

The calculations were performed on a BÉSM-6 computer for a high-current electron beam with a radius R = 0.1-0.2 cm, current $I = 10^3$-10^6 A, and electron energy E_0 = 1-5 MeV for normal incidence of the beam on a semiinfinite target consisting of Al, Cu, or Au. The program per-

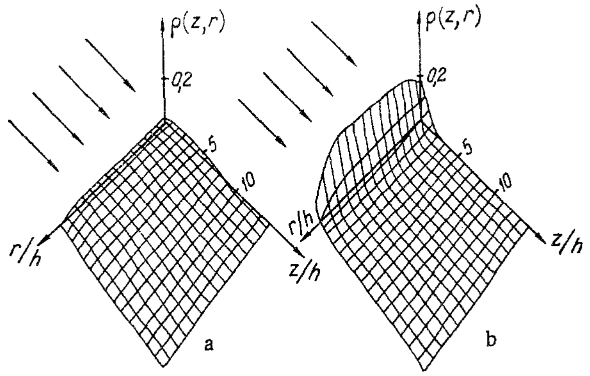

Fig. 1. Spatial distribution of energy losses in aluminum for E_0 = 1 MeV, N = 1000, D = 0.4 cm: a) for I = 10^3 A; b) 10^6 A; $\rho(z, r) = (\pi h^3/P_0)(dP/dV)$.

mitted fixing the energy losses, the currents, and the magnetic fields in each cell of the region studied.

Figure 1, constructed with the help of the "Grafor" program, shows the results of the calculation of the spatial distribution of the energy losses in a semiinfinite Al target. The left side of the figure refers to a low-current beam (I = 10^3A), while the right side refers to a high-current beam (I = 10^6 A). The arrows indicate the direction of the incident beam; the linear size of a cell corresponds to one-half the grid step h. The figure reflects quite clearly the effect of the characteristic magnetic field on the beam: the region of energy release for HCEB is compressed toward the surface in such a way that for I = 10^6 A its characteristic size in depth decreases almost by an order of magnitude, while the values of the density of the energy loss in this region correspondingly increase by almost an order of magnitude.

Figure 2 shows the results of the calculation of the energy losses in a semiinfinite target as a function of the current strength and the diameter of the electron beam. the relative released power density $\rho(z) = (h/P_0)(dP/dz)$ (P = IU, U is the accelerating voltage in MV, numerically equal to the electron energy in MeV) is plotted along the ordinate axis and the depth is plotted along the abscissa axis in fractions of the electron range r_0. For each sample, curve 1 corresponds to a low-current beam (I = 10^3 A), when the effect of the characteristic magnetic field can be neglected. The remaining curves were constructed for HCEB: curve 2 corresponds to I = 10^5 A, R = 0.2 cm; curve 3 corresponds to I = 10^6 A, R = 0.2 cm; and curve 4 corresponds to I = 10^6 A, R = 0.1 cm. All calculations were performed for electrons with an initial energy E_0 = 1 MeV.

One can see from the figure that the characteristic magnetic field of the HCEB sharply changes the graph of the energy release, compressing it toward the surface and significantly increasing the density near it. The ratio of the electron range r_0 to the Larmor radius can serve as a characteristic of the effect of the characteristic magnetic field:

$$r_L = \frac{m_e v \gamma}{eB}.$$

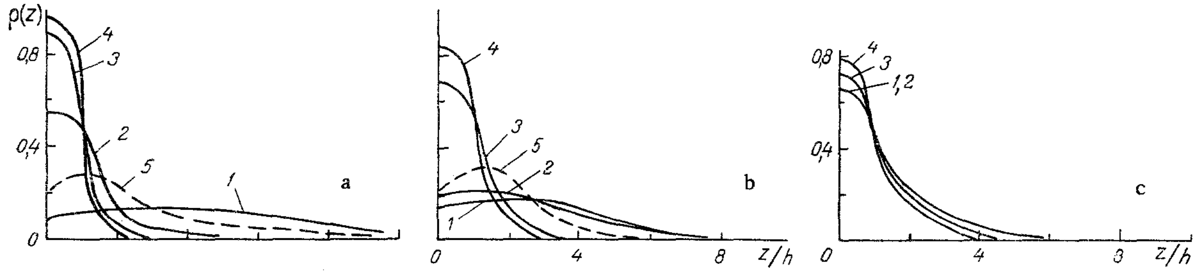

Fig. 2. Distribution of energy losses of the beam over the thickness of the aluminum (a), copper (b), and gold (c) samples: 1) for I = 10^3 A; 2) I = 10^5 A, R = 0.2 cm; 3) I = 10^6 A, R = 0.2 cm; 4) I = 10^6A, R = 0.1 cm; 5) from [6].

As the order number of the element increases the range r_0 and together with it the ratio r_0/r_L decreases (for dia- amd paramagnets r_L is virtually independent of the material) and therefore the effect of the characteristic magnetic field on the character of the energy release becomes weaker. The broken curve 5 was constructed in [6] for the same values of I, E_0, and R as those used for curve 3. The differences in the results are attributable to the fact that for the step size s chosen in [6] ($\Delta E = 0.05E$) the condition that the effective angle of deflection in the magnetic field be limited ($b < 1$ rad) is not satisfied ($b \approx 2.5$ rad).

The calculations showed that as the electron energy E_0 increases the character of the self-consistent distribution of the energy release in range units remains virtually unchanged. This is attributable to the fact that in the energy range studied (1-5 MeV) the ratio r_0/r_L is practically constant.

LITERATURE CITED

1. A. F. Akkerman, Yu. M. Nikitushev, and V. A. Botvin, Monte Carlo Solution of Problems of the Transport of Fast Electrons in Matter [in Russian], Alma-Ata (1972).
2. G. E. Gorelik and S. G. Rozin, Inzh.-Fiz. Zh., 22, No. 6, 1110-1113 (1972).
3. L. I. Rudakov, Fiz. Plazmy, 4, 72-77 (1978).
4. K. Imasaki, S. Miyamoto, and S. Higaki, Phys. Rev. Lett., 43, No. 26, 1937-1940 (1979).
5. R. Miller, Introduction to the Physics of Strong-Current Beams of Charged Particles [in Russian], Moscow (1984).
6. V. I. Boiko, E. A. Gorbachev, and V. V. Evstigneev, Fiz. Plazmy, 9, No. 4, 764-769 (1983).
7. A. S. Roshal', Stimulation of Charged Beams [in Russian], Moscow (1979).

GRADIENT OF THE DISCREPANCY IN THE ITERATIVE SOLUTION OF INVERSE HEAT-CONDUCTION PROBLEMS. III. CALCULATION OF THE GRADIENT USING A CONJUGATE BOUNDARY PROBLEM

O. M. Alifanov and S. V. Rumyantsev

UDC 536.24

The determination of the gradient in the discrepancy functional, which is required for the construction of regularizing gradient algorithms for their solution, is considered for various formulations of nonlinear inverse problems of generalized heat conduction.

In [1], the conditions of the conjugate boundary problems were derived for the formulation of the second and third boundary problems in the case of a quasilinear generalized heat-conduction equation, and formulas were obtained for determining the discrepancy gradient in terms of the conjugate variable. It was assumed that the time dependence of the temperature at one mobile internal point of a one-dimensional spatial region is known as the initial data.

Below, the conjugate problem is brought to a form in which there is no singular term, the conjugate problem is formulated for the case of measurements at the boundary of the region, and expressions are obtained for the discrepancy gradient in measurements at several spatial points and also for other types of boundary conditions of the problem.

As in [1], the gradient of the discrepancy functional $J = \frac{1}{2}\int_0^{\tau_m} [T(d(\tau), \tau) - f(\tau)]^2 d\tau$ with respect to the functions $\xi(x)$, $p_1(\tau)$, $p_2(\tau)$, and the numercial vectors $\bar{\lambda} = \{\lambda_j\}_1^{M_1}$, $\bar{C} = \{C_j\}_1^{M_2}$, $\bar{K} = \{K_j\}_1^{M_3}$, $\bar{g} = \{g_j\}_1^{M_4}$ is considered, for the following conditions

$$CT_\tau = (\lambda T_x)_x + KT_x + g,$$
$$(x, \tau) \in Q_\tau = \{X_1(\tau) < x < X_2(\tau), \quad 0 < \tau < \tau_m\};$$

S. Ordzhonikidze Moscow Aviation Institute. Translated from Inzhenerno-Fizicheskii Zhurnal, Vol. 52, No. 6, pp. 981-986, June, 1987. Original article submitted January 6, 1986.

0022-0841/87/5206-0708 $12.50